JOURNAL OF SPACECRAFT AND ROCKETS
Vol. 32, No. 6, November–December 1995

Transpiration Cooling Effects on Nozzle Heat Transfer and Performance

D. Keener,* J. Lenertz,† R. Bowersox,‡ and J. Bowman§
U.S. Air Force Institute of Technology, Wright–Patterson Air Force Base, Ohio 45433

The effects of transpiration cooling on boundary-layer growth, heat transfer, and nozzle performance were investigated. A two-dimensional Mach 2.0 contoured nozzle ($Re/m = 5.2 \times 10^7$), with one contoured wall constructed of sintered stainless steel (2.0-μm pore size) was tested. Blowing ratios up to 0.51% of the freestream mass flow were tested using high-frequency-response heat flux and pressure instrumentation. Measurements included wall heat flux and static pressure, as well as exit pitot pressure profiles. Shadowgraph photography was used for flow visualization. A reduction in heat transfer of up to 14% was measured for the highest blowing ratio. On the other hand, large increases in the nozzle exit boundary-layer thickness were found. However, blowing had a minimal effect on the nozzle thrust coefficient and specific impulse. In general, this study highlighted the potential beneficial and adverse effects of transpiration cooling on rocket nozzle cooling.

Nomenclature

A	= area
B_s	= heat-flux blowing ratio
C_F	= thrust coefficient
D	= diameter
H_e	= nozzle exit height
h	= heat transfer film coefficient
I_{sp}	= specific impulse
M	= Mach number
Pr	= Prandtl number
p	= pressure
Re_{D^*}	= $\rho^* u^* D^*/\mu_0$
r_c	= throat radius of curvature
St_{RN}	= rocket nozzle Stanton number
s	= arc length along porous material
δ	= velocity boundary layer thickness
δ^*	= displacement thickness
μ	= dynamic viscosity
ρ	= density

Subscripts

e	= exit
i	= injection
o	= total condition
0	= nonblowing case

Superscripts

C	= centerline
0	= nonblowing case
δ^*	= based on area-ratio reduction
$\bar{}$	= average value
$*$	= throat condition

Received March 6, 1995; revision received July 5, 1995; accepted for publication July 6, 1995; presented as Paper 95-2497 at the AIAA/ASME/SAE/ASEE 31st Joint Propulsion Conference and Exhibit, San Diego, CA, July 10–12, 1995.

*Research Assistant, Aero/Astronautical Engineering Department. Member AIAA.
†Research Assistant, Aero/Astronautical Engineering Department.
‡Assistant Professor, Aero/Astronautical Engineering Department. Member AIAA.
§Lt. Colonel, U.S. Air Force; Associate Professor, Aero/Astronautical Engineering Department. Senior Member AIAA.

Introduction

RENEWED interest in liquid-propellant space launch vehicles has sparked research to improve the performance of these systems. Nozzle heat transfer and material thermal limitations remain a limiting factor in the performance of modern rocket engines. Actively cooled rocket nozzles allow the high combustion temperatures necessary for high performance while maintaining the structural integrity of the nozzle. Several methods of active cooling have been employed to address this problem, including regenerative, film, and transpiration cooling.

Regenerative cooling involves pumping a liquid through channels surrounding the outside of the combustion chamber. This method has been used extensively because of its simplicity and low cost. Also, the heat absorbed by the coolant is often not wasted, because it augments the initial energy content of the propellant prior to injection, increasing the exhaust velocity slightly.[1] One drawback to regenerative cooling is the additional pumping required to force coolant through the coolant lines.

Film cooling involves injecting low-temperature gas or liquid through one or several discrete holes in a nozzle wall to establish a protective film on the surface. Since the coolant is inside the thrust chamber, it accepts heat directly, which makes it potentially a more effective cooling method than regenerative cooling. In addition, it is relatively easy to implement and has been used in thrust chambers for many years.[1]

In a performance study by Azevedo,[2] film cooling was utilized in a convergent–divergent nozzle, and the effects on the nozzle thrust efficiency were measured. The parameters investigated in that study included injection angle (15–100 deg), nozzle divergence angle (1–10 deg), and blowing ratio (1–8%). In general, the losses were on the order of 1–5%. The drawback of film cooling is that it requires large injection mass flow rate per unit area (10–300% of mainstream flow), which can cause thrust losses due primarily to flow disturbances. The injection velocities of transpiration cooling are typically much lower than those of film cooling. Thus, it is expected that the losses will be smaller than those associated with film cooling.

Transpiration cooling is essentially the limiting case of film cooling because it involves pushing gas or liquid uniformly through an area of porous wall material.[1] Ideally, it can be thought of as using an infinite number of film cooling ports with zero distance between them. This cooling technique has been successfully used for cooling injector faces in the upper stage engine (J-2) of the moon launch vehicle and the Space Shuttle main engines, but it has not been used for cooling the thrust chamber or nozzle regions of large rocket engines.[1]

In general, analytical relations are not available to predict the effects of transpiration or film cooling on heat flux or boundary-layer growth in configurations with a pressure gradient, which is the case

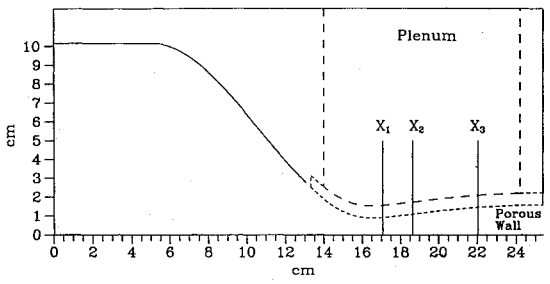

Fig. 1 Schematic of Mach 2.0 contoured nozzle with a sintered stainless steel floor.

in supersonic nozzles.[3] However, it is expected that a heat transfer rate reduction similar to or better than for film cooling can be realized, with decreased flow disturbances, indicating that transpiration cooling could be a more attractive method than film or regenerative cooling. Therefore, this investigation proposes to study the effects of transpiration cooling in a supersonic nozzle on boundary-layer growth, heat transfer, and performance at low blowing ratios.

The objective of this research was to investigate the differences between flow over a porous and a nonporous wall with no blowing. In particular, the effect of blowing ratio on boundary-layer thickness, Mach-number profile across the exit of the nozzle, and nozzle heat transfer characteristics were studied. These objectives were accomplished with a shock-tube study of a two-dimensional, Mach 2.0 (exit $Re/m = 5.2 \times 10^7$) nozzle, where one of the contours was constructed from porous material. The sintered steel portion of the contour started just upstream of the throat (see Fig. 1 for a schematic of the present model), using air as the primary and injected fluid.

Background: Boundary-Layer Characteristics

The current state of knowledge about turbulent boundary layers over porous plates with injection or suction has not advanced to the same state as that of turbulent flow over solid walls.[4] Additional complications associated with the present study include compressibility and pressure gradient. However some low-speed flat-plate data are available, and the overall trends noticed in these studies were used to guide the expectations for the present research. For example, transpiration has been shown to cause significant increases in the boundary-layer thickness. On the other hand, Antonia and Fulachier[5] found that the boundary-layer thickness decreased in the presence of suction. A study,[6] which involved injecting air into air through a section of porous material on a flat plate, showed a rapid increase in boundary-layer thickness right at the beginning of the porous material, with slower increases further downstream. Finally, as pointed out by both Schetz[4] and White,[7] porous walls without injection or suction will cause greater skin friction than impermeable walls, most likely as a result of roughness. In addition, Schetz[4] shows that the increase in skin friction (for the nonblowing case) over the smooth wall at the same conditions for a sintered plate is lower than that for a perforated plate. Presumably, this is a result of the smaller roughness associated with the sintered plate. Thus, it can be reasonably expected, based on their observation and the Reynolds analogy, that the heat transfer will also increase in the presence of the porous material.

Bartz,[8] in order to estimate the heat transfer in convergent–divergent nozzles, developed the following relation for the film coefficient:

$$St_{RN} \equiv \frac{h_0}{\rho^* u^* C p_o} = 0.026 Re_{D^*}^{-0.2} Pr_o^{-0.6} \left(\frac{D^*}{r_c}\right)^{0.1} \left(\frac{A^*}{A}\right)^{0.9} \sigma \quad (1)$$

where the asterisk indicates conditions at the nozzle throat, and σ is defined by

$$\sigma = \left\{\left[0.5\left(\frac{T_w}{T_o}\right)\left(1 + \frac{\gamma - 1}{2} M^2\right) + 0.5\right]^{0.65} \times \left(1 + \frac{\gamma - 1}{2} M^2\right)^{0.15}\right\}^{-1} \quad (2)$$

where for the present shock tunnel, T_w was very nearly the ambient room temperature, since the wall temperature does not change appreciably during the nominally 1.5-ms test. One goal of this research was to modify this relation, incorporating a blowing parameter to allow prediction of heat transfer coefficient with transpiration cooling.

Experimental Apparatus

Facilities

A Mach 2.0 characteristic contoured nozzle was designed, fabricated, and installed in the AFIT low-pressure shock tube. The two-dimensional nozzle contour was designed for uniform exit flow of air, using the method of characteristics. A double-reflection expansion was used in order to keep the initial expansion angle low (6.59 deg). An incompressible boundary-layer correction was applied to the supersonic contour. The subsonic contraction was designed for a smooth transition from the shock-tube cross section (10.16 × 20.32 cm) to the nozzle throat (10.16 × 1.87 cm). The contour shown in Fig. 1 was the result of the nozzle design process. The exit height was 3.25 cm. Thus, the exit width-to-height aspect ratio was 3.13. A 0.18-mm-thick Mylar® diaphragm was used to separate the high-pressure section from the low-pressure section, and the tunnel was operated with an air–helium driver mixture at 581 kPa. The driven section contained 98-kPa air. The tunnel was operated in shock reflection mode; thus, the stagnation pressure and temperature for the nozzle were measured at approximately 482±35 kPa and 475±10 K, respectively.

Model

The model used for this experiment was the two-dimensional, Mach 2.0 method of characteristics contoured nozzle (exit $Re/m = 5.2 \times 10^7$). Although it is not entirely representative of axisymmetric rapid-expansion rocket nozzles, the two-dimensionality and modest expansion of the present nozzle was well suited for adaptation for transpiration cooling. One side of the nozzle was modified for blowing, whereas the other remained solid (the nonblowing side).

Four layers of 1.59-mm-thick 316L sintered stainless steel made from 2.0-μm beads were installed on the blowing side of the nozzle. The porous material started 1.27 cm upstream of the throat, and extended to the exit. Each layer of porous material was shaped to the nozzle individually to minimize unevenness where the porous material met the solid aluminum. A plenum chamber was used to drive the injectant gas through the porous nozzle wall (see Fig. 1).

Instrumentation

The run times in the shock tube were very short (≈1.5 ms); hence, high-frequency-response pressure transducers and heat-flux gauges were required for data collection. Pressure transducers and heat-flux gauges were placed in pairs along the nozzle walls. Also, pressure transducers were placed in the subsonic section, in the injection plenum, in a pitot probe at the nozzle exit, and along the top of the shock tube upstream of the nozzle. See Fig. 1 for the downstream instrumentation locations.

Test Matrix

Five blowing-ratio data sets were collected during this experiment. The plenum pressure was used to control the blowing ratio. Five to seven trials per flow condition were acquired. The local blowing ratio, which represented the total averaged ratio of injection to nozzle exit mass flow rate per unit area, was defined as

$$B_s = \frac{1}{\rho_{\infty,s} u_{\infty,s} S} \int_0^s \rho_i u_i \, ds \quad (3)$$

The ratio of injection to nozzle mass flow rate can be found by multiplying B_s by the ratio of injection to nozzle exit areas. The injectant mass flow rate was estimated from the manufacturer's mass-flow-rate–pressure-drop charts.[9] The relations were verified for the present experiment. For the lower injectant plenum pressures, a portion of the porous material experienced suction. This suction was due to the pressure variation along the nozzle. At the lower gas injection pressures, the possibility existed for the pressure in the

Table 1 Total positive blowing ratio

Test case	Plenum pressure, kPa	Blowing ratio, %	Error, %
0	99.0	0.013	7.2
1	255.0	0.46	4.2
2	310.0	0.77	1.7
3	345.0	0.99	6.9
4	380.0	1.12	4.3

nozzle to be greater than the gas injection pressure, especially upstream from the nozzle throat, where the nozzle static pressure was greatest. This lower pressure would result in suction in the upstream portion of the nozzle and sometimes into the throat region. As the nozzle pressure dropped below the gas injection pressure, injection was observed.

To estimate the blowing ratio, Eq. (3) was numerically integrated. The total positive blowing ratio for the five test conditions was obtained by integrating Eq. (3) from the point where positive injection was first encountered along the nozzle to the end of the porous wall. Table 1 summarizes the positive blowing ratios for the present experiment. The errors in Table 1 were estimated from an unbiased standard deviation over a series of five to seven runs. All subsequent data are referenced to the local blowing parameter evaluated by integrating Eq. (3) from the beginning of the porous wall (suction included) to the local position.

Data Reduction

Shadowgraphs were acquired during the initial phase of the experiment to characterize the flowfield in the nozzle and to provide boundary-layer thickness information. The boundary-layer thickness was estimated using a caliper micrometer. Average values over the five to seven trials were used to define the boundary-layer thickness. In general, the results were found to be repeatable to within about 10–15%.

Heat-flux gauges (more accurately referred to as thin-film resistance thermometers) were used to measure variations in surface temperature through changes in the resistance of the film. By using basic heat transfer relations, the surface temperature history can be used to determine heat transfer to the surface of a gauge.

If the substrate of the gauge is assumed to be a semi-infinite slab, and if the film of platinum is assumed to be so thin that it does not affect the temperature history of the surface of the substrate, then the relation between the temperature history of the gauge and the heat flux imparted to the surface can be obtained[10]:

$$q''(t) = \sqrt{\frac{\rho ck}{\pi}}\left(\frac{T(t)}{\sqrt{t}} + \frac{1}{2}\int_0^t \frac{T(t) - T(\tau)}{(t-\tau)^{\frac{3}{2}}}\,\mathrm{d}t\right) \tag{4}$$

where the parameter $\sqrt{\rho ck}$ is called the thermal product. The thermal product of each gauge was found using an electrical-heating calibration technique.[10] In addition, the heat-flux gauges were mounted on a flat plate. They were then subjected to an equal heat flux, and a weighted averaging technique was used to force the gauges to yield equal heat transfer coefficients.

Equation (4) has a singularity at $t = \tau$, which will cause errors in the value of q''. Therefore, this relation was modified to allow an accurate numerical integration.[11] The resulting summation can be further simplified by noticing that when $t = 0$, the output of the gauge is zero:

$$q''(t_J) = 2\sqrt{\frac{\rho ck}{\pi}}\sum_{j=1}^{J}\frac{T(t_j) - T(t_{j-1})}{\sqrt{t_J - t_j} + \sqrt{t_J - t_{j-1}}} \tag{5}$$

Heat-flux and heat transfer coefficient histories were calculated by numerically integrating Eq. (5) using the thermal product and temperature history of the gauge. The errors associated with the present technique are generally accepted to be ±5–10% of the measured value. The present data were found to be repeatable to within about 7.5%.

Exit Mach-number profiles were obtained by placing a pitot probe at different positions across the exit plane. At each location, the pitot and upstream data were averaged over the run time, and the Mach number was calculated from the total pressure ratio (p_{02}/p_{01}) with the usual relations for a compressible thermally and calorically perfect gas. Allowing for transducer calibration errors and an expected 5–15% freestream turbulence, the estimated uncertainty in the total-pressure ratio at Mach 2.0 was about[12] 2.7%, which implied a 2.0% error in the measured exit Mach number.

Results and Discussion

Results Without Blowing

The nonblowing side of the nozzle provided reference heat-flux data (no transpiration cooling) throughout the testing. It was assumed here that blowing on one wall would not significantly affect the boundary layer on the other wall. This assumption seems reasonable for the low blowing ratios used in the present study, and it was validated for the present experiment (discussed in the Results with Blowing subsection). Because of the pressure gradient along the nozzle and the constant pressure within the transpiration plenum, the blowing side of the nozzle could never truly be used to measure nonblowing heat flux. This lack of injection control through porous material is a major objection to transpiration cooling.[13] However, since the present study was investigating the effects of transpiration cooling, this was not considered a limitation here.

During a firing of the shock tube, the interaction between the shock and the nozzle had a strong influence on the measured values of the heat transfer coefficient. When the shock moved down the tube, most of it was reflected by the converging portion of the nozzle, creating the stagnation conditions. A fraction of the shock was not reflected, and was hence swallowed by the nozzle.

The nonreflected portion of the original shock expanded in and reflected off the diverging section of the nozzle. The passage of the ensuing oblique shocks and turbulent flow over the heat-flux gauges caused a rapid rise in heat flux (see Fig. 2). Following the initial jump, there was a fairly quick drop to the steady-flow run-time heat flux, followed by a slow, steady dropoff to near-zero flux at the time the nozzle unstarted.

The reason behind this heat-flux behavior is related to the nature of the boundary layer. In nozzle flow, the boundary layer acts as a thermal insulator. A thick boundary layer will tend to be a better insulator than a thin boundary layer. Until the first shock wave passed over the heat flux gauge, there had been no flow and therefore no boundary layer, so that the heat flux quickly reached a maximum. Following the passage of the shock, the boundary layer grew and began to insulate the nozzle walls. Once steady flow had been achieved and the boundary layer was fully developed, the heat flux was found to decrease slightly because the wall temperature increased during a run. The beginning and end of the steady-flow run time (0.65 and 2.0 ms) were established from pressure transducer data and shadowgraphs of the nozzle.

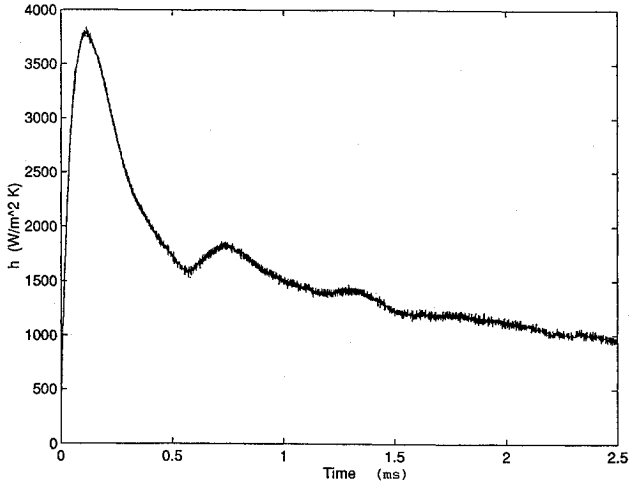

Fig. 2 History of nozzle heat transfer coefficient.

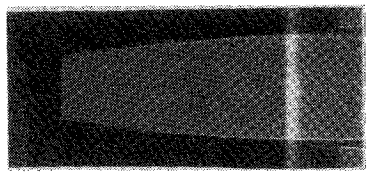

a) Blowing 0

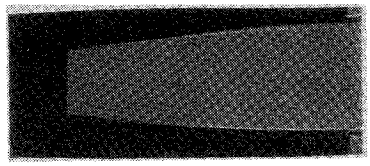

b) Blowing 1

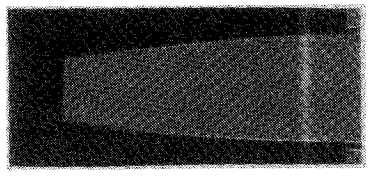

c) Blowing 2

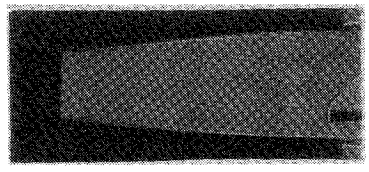

d) Blowing 3

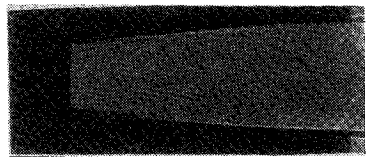

e) Blowing 4

Fig. 3 Shadowgraphs showing boundary-layer growth with blowing (blowing along upper wall).

Results with Blowing

Shadowgraph visualization of the boundary layer at each blowing level was the first indication that transpiration cooling had an effect on boundary-layer thickness. Figure 3 shows a series of shadowgraphs for each blowing level. Notice that the boundary layer on the nonblowing wall appears to be unaffected by blowing for all of the test cases. This result validates the assumption (discussed in the "Results Without Blowing" section) concerning the use of the opposite wall nonblowing data as a comparison. The increase in boundary-layer thickness on the blowing side with increasing blowing is clearly visible. All other visible features of the flow except the boundary-layer thickness appear to be unchanged in each case. This lack of change indicated that the disturbance due to transpiration is limited to the boundary-layer region of the flow.

Boundary-layer growth data along the nozzle did not show a jump in thickness at the beginning of the porous material as was reported by Goldstein et al.[6] For their work, a flat plate with no pressure gradient was studied; hence, constant blowing over the entire porous section was present. When the flow interacted with the injection, there was a significant jump in boundary-layer thickness. With the pressure gradient present, the gas injectant velocity starts small and increases along the porous area. This gradual increasing velocity caused smooth boundary-layer growth along the length of the nozzle. Figure 4 shows the boundary-layer height along the nozzle for all of the test cases, including the nonblowing wall. The boundary-layer thicknesses at the nozzle exit are included in Table 2.

To determine the effectiveness of transpiration cooling, heat-flux data were acquired on both the blowing and nonblowing sides of the nozzle for the five test cases. Because of gauge attrition, heat-flux gauges were positioned at only stations 1 and 2 (see Fig. 1 for station location).

Table 2 Nozzle performance results

Case	$2\delta/H_c$	$\bar{M}_c$	M_c^C	M_c^δ	C_p/C_{p-1}, %
Non.	0.03	—	—	1.99	−0.0
0	0.10	1.89	1.92	1.94	−0.6
1	0.12	1.88	1.91	1.94	−0.5
2	0.13	1.86	1.88	1.94	−0.4
3	0.14	1.86	1.90	1.94	−0.3
4	0.15	1.85	1.88	1.94	−0.2

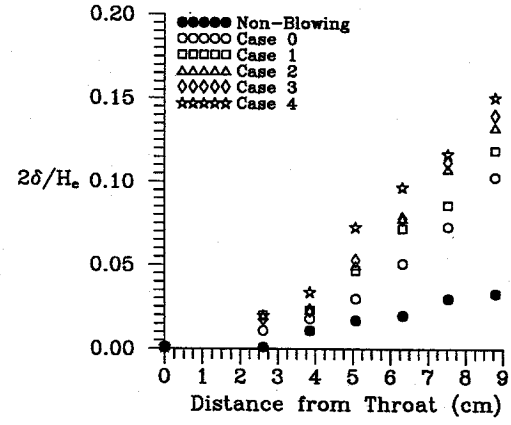

Fig. 4 Effects of blowing on nozzle boundary-layer growth.

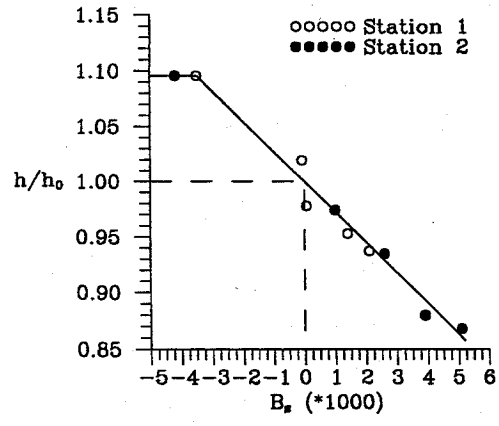

Fig. 5 Blowing effects on heat transfer coefficient.

The blowing-side heat transfer film coefficients were normalized with the corresponding nonblowing-side coefficients. The results are plotted against the blowing ratio in Fig. 5. It is important to note here that the blowing ratios shown in Fig. 5 include suction. As can be seen, for the lowest total blowing ratios, some of the gauges were located in a region of suction. Open data points represent position 1, and filled data points represent position 2. The corresponding freestream Mach numbers were 1.17 and 1.54, respectively. As can be seen in Fig. 5, there does not appear to be a significant difference in the cooling effectiveness at the two locations in the nozzle. The overall slope is a linear best fit with a standard deviation of 0.63%. The upper horizontal line represents a limiting heat flux after the boundary-layer thickness has been reduced to a minimum by suction. These data allow the following simple modification to Eq. (1):

$$h = (1 - 27.38B_s)h_0 \tag{6}$$

where B_s is given by Eq. (3). Figure 6 compares the predictions of Eq. (6) with the present data. As can be seen, the agreement is excellent.

Uniformity of the exit flow is an important performance parameter. Boundary-layer growth with injection has already been shown, which means there was a larger mass-flow defect region

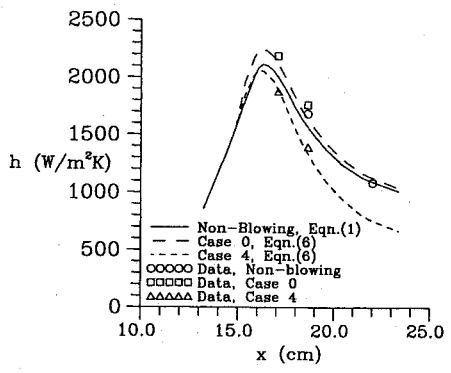

Fig. 6 Comparison of predicted results and data.

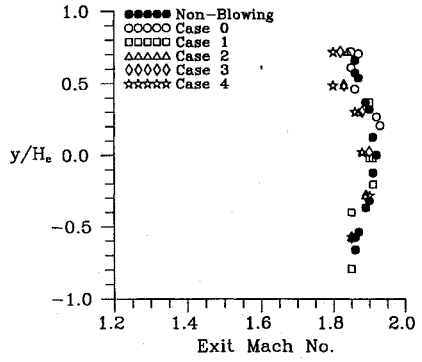

Fig. 7 Effects of blowing on the exit Mach-number profile.

in the boundary layer. Therefore, more of the flow energy had to be spent to accelerate the very low-velocity injected gas and overcome this defect. This loss of energy was expected to degrade the exit Mach number, especially near the wall. Larger injection rates caused greater disturbances to the flow. For transpiration to be an attractive method of cooling high-temperature nozzles, this effect must be characterized.

Figure 7 compares the exit Mach profiles for each case with an idealized nonblowing case. This case was obtained by mirroring the exit profile on the nonblowing side to the blowing side for the lowest blowing ratio. As can be seen, the effects of transpiration on the exit Mach number were relatively small in this study: 2% reduction in overall average Mach number, and 3.5% reduction in the blowing region. The maximum spatial variation in Mach number was found to be about 4.5%. Table 2 includes the average exit Mach numbers, the centerline Mach number, and the Mach numbers estimated from the decrease in exit area due to the boundary-layer growth. Note that it was assumed that for the very low blowing ratios used here the $\frac{1}{7}$-power law would adequately describe the boundary-layer profile; thus $\delta^*/\delta \approx \frac{1}{8}$.

These results validated the expectation that transpiration would decrease the exit Mach number of the nozzle. In addition, the results showed that the effect of transpiration was practically limited to the blowing-side region of the flow, again reinforcing the validity of using the nonblowing side for comparison. As expected, the decrease in exit Mach number coupled with the slight increase in mass flow rate had a very small adverse effect on the performance of the nozzle in terms of thrust coefficient (see Table 2). Note that the change in mass flow through the nozzle, including suction, was included in the estimation of the thrust coefficient C_F. For the present study $I_{sp}/I^0_{sp} \approx C_F/C^0_F$, where $I^0_{sp} = 59.24$ s and $C^0_F = 1.078$ for the conditions associated with the first row of Table 2.

It is important to note that the performance losses were based on the effects of transpiration over the entire nozzle wall. The heat transfer measurements were obtained well upstream of the exit in a region of low blowing compared to that near the exit. Thus the performance results are somewhat pessimistic with regard to the amount of heat transfer reduction. In any event, the present study was able to show that transpiration cooling provided significant reductions in heat transfer for very minimal losses in performance.

Conclusions

The effects of transpiration cooling at low blowing ratios on the heat transfer and nozzle performance were investigated on a two-dimensional contoured nozzle. Overall, the heat transfer rate was shown to be significantly reduced by transpiration cooling. A 14% reduction was measured for a local blowing ratio of 0.51%. The specific-impulse and thrust-coefficient losses, however, were minimal (less than 0.6%). Nevertheless, the average exit Mach number was reduced by 2.0%, and the uniformity of exit flow was noticeably affected, with up to a 4.5% variation in Mach number. The exit boundary-layer thickness increased by as much as 400% over the investigated range of blowing ratios.

In conclusion, the present two-dimensional results have indicated that transpiration cooling has the potential to be an effective means of rocket nozzle cooling.

References

[1]Sutton, G. P., *Rocket Propulsion Elements*, 6th ed., Wiley, New York, 1992, pp. 289–294.

[2]Azevedo, D., "Measured Thrust Losses Associated with Secondary Air Injection Through Nozzle Walls," *Journal of Propulsion and Power*, Vol. 9, No. 1, 1993, pp. 43–50.

[3]Beitel, G. R., "Boiling Heat Transfer Processes and Their Application in the Cooling of High Heat Flux Devices," Arnold Engineering Development Center, AEDC-TR-93-3, Arnold AFB, TN, June 1993.

[4]Schetz, J. A., *Foundations of Boundary Layer Theory for Momentum, Heat, and Mass Transfer*, Prentice–Hall, Englewood Cliffs, NJ, 1984, pp. 139–219.

[5]Antonia, R. A., and Fulachier, L., "Topology of a Turbulent Boundary Layer With and Without Wall Suction," *Journal of Fluid Mechanics*, Vol. 198, 1989, pp. 429–451.

[6]Goldstein, R. J., Shavit, G., and Chen, T. S., "Film Cooling Effectiveness with Injection Through a Porous Section," *Journal of Heat Transfer*, Vol. 87, No. 3, 1965, pp. 353–360.

[7]White, F. M., *Viscous Fluid Flow*, 2nd ed., McGraw–Hill, New York, 1991, pp. 394–499.

[8]Bartz, D. R., "A Simple Equation for Rapid Estimation of Rocket Nozzle Convective Heat Transfer Coefficients," *Jet Propulsion*, Vol. 27, No. 1, 1957, pp. 49–51.

[9]Mott Metullurgical Corp., *Technical Handbook for Precision Porous Metal Products*, Product Catalog No. 1000A, Farmington, CT, 1986.

[10]Schultz, D., and Jones, T., *Heat Transfer Measurements in Short Duration Hypersonic Facilities*, AGARDograph AG-165, Feb. 1973.

[11]Cook, W., and Felderman, E., "Reduction of Data from Thin-Film Heat-Transfer Gages: A Concise Numerical Technique," *AIAA Journal*, Vol. 4, No. 3, 1966, pp. 561, 562.

[12]Volluz, R. J., *Handbook of Supersonic Aerodynamics, Section 20, Wind Tunnel Instrumentation and Operation*, Ordnance Aerophysics Lab., NAVORD Rept. 1488 (Vol. 6), Dangerfield, TX, Jan. 1961.

[13]May, L. R., and Burkhardt, W. M., "Transpiration Cooled Throat for Hydrocarbon Rocket Engines," NASA CR 8-36952, Dec. 1991, pp. 1–53.

K. J. Weilmuenster
Associate Editor